
An Attribute-Based Measure of Video Complexity

Aditya Sarkar¹, Yi Li^{2,†}, Zihao Wang⁴, Jiacheng Cheng³, Sai Vidyaranya Nuthalapati⁴

Aashu Singh⁴, Shlok Kumar Mishra⁴, David Jacobs¹, Nuno Vasconcelos²

¹UMIACS-University of Maryland College Park, ²University of California San Diego,

³Yale University, ⁴Meta AI

Abstract

A new framework for the estimation of the complexity posed by video-question pairs to video-LLMs, *Video Attribute-Based Complexity* (VideoABC), is proposed. Video complexity is defined as the probability of failure of a video-LLM for a given video-question pair. VideoABC is a non-parametric complexity measure, using a reference video dataset and a pre-defined vocabulary of video attributes informative of complexity, *e.g.* the scene complexity or the speed of the video event informative of the question. In a training phase, reference videos are projected into the space of these attributes, which is then quantized. The expected ABC of each quantization cell is then computed. Given a new video and its projection into the attribute space, complexity is estimated by the expected ABC of the associated quantization cell. To enable the use of VideoABC with small reference video datasets, two quantizers are combined: a k-means quantizer that enables accurate complexity estimates for samples in the distribution of the reference dataset and a universal lattice quantizer that guarantees generalization to out-of-distribution samples. A synthetic video generation procedure, inspired by target-distractor manipulations of psychophysics studies, is proposed to populate the cells of the lattice quantizer during training, enabling the computation of their expected ABCs. Experimental results show that VideoABC is effective even with very low-dimensional attribute representations, substantially outperforming approaches like ‘video-LLM as judge’ with much less complexity. Finally, the explainable nature of the VideoABC score, in terms of well-defined attributes, is shown to provide insights on how the attribute composition of benchmarks affects their complexity.

1 Introduction

In recent years, there have been significant advances in Large Language Models for video (video-LLMs) [62, 66, 7], namely in areas like video-question answering [65, 29, 60]. However, these models are expensive and far from perfect. An important open question for the development of both better models and more effective applications is to how to predict the probability of failure of a video-LLM for a particular video-question pair. In this work, we refer to this probability as a measure, or score, of video complexity. In the absence of complexity measures, even the simple task of benchmarking model performance can be extremely inefficient. For example, [67, 16] report that the 184 A100 GPU hours required to evaluate a small (3B-parameter) model across all existing benchmarks are mostly spent on video-question pairs answerable by an LLM without video input, providing no insight about the video representation. This has motivated the research community to compute complexity of video-question pairs and test models only on those that are hard [17].

Existing approaches to estimating complexity [40, 45] are usually parametric, relying on model, typically an LLM, to produce a holistic complexity score. For example, [21] measures video complexity by counting the number of reasoning steps a video-LLM takes to answer a question. Similarly, [14] proposes generating executable code with an LLM to solve the query and uses this

[†]Work done at UC San Diego. Currently working at Qualcomm.
Preprint.

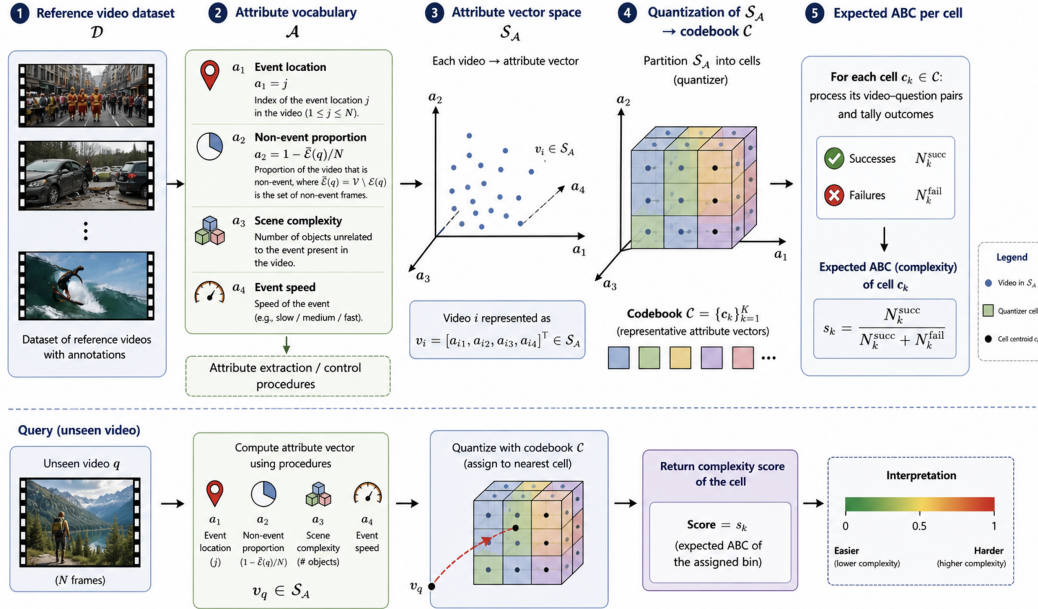


Figure 1: VideoABC is an approach for the characterization of video-question complexity in terms of a set of video attributes. Top: 1) given a reference video dataset, 2) a set of predefined attributes \mathcal{A} is extracted, to 3) project each video into an attribute vector space that 4) is vector quantized. 5) the expected ABC of each cell is finally computed by measuring model success/failure rate for its videos. Bottom: to characterize complexity, an unseen video-question pair is first quantized in attribute space, and the expected ABC of the resulting cell returned as a complexity score.

process as a proxy for difficulty. However, these approaches have several limitations. First, they do not utilize video attribute to determine its complexity. It is well-known in literature that attributes determine complexity [29, 60, 65] *e.g.* a long video or a video with fast event is complex. Yet existing complexity models do not rely on them to determine their score resulting in these methods offering limited diagnostic value. Second, they are computationally inefficient. There are many applications where it would be useful to obtain a complexity score *before* the video is processed by the video-LLM. In fact, a common approach to evaluate model performance, usually referred to as *LLM-as-judge* (denoted Judge in this work) is to rely on an external model to evaluate the performance of the target model [14, 40]. While these approaches can produce complexity scores, effective performance usually requires Judge models much larger and complex than the target model, typically proprietary models like GPT [1] or Gemini [39]. Such a model may be infeasible in applications where computational resources are limited. Thus there is a pressing need for complexity scores that are interpretable, predictive and computationally efficient.

We argue that the problem has two main causes. The first is the reliance on *parametric* scores of complexity. Given the complexity of predicting video-LLM failures, it is hard to see how this can be done by a model smaller than the target video-LLM. One possibility is to build small parametric extensions that leverage features of the intermediate target video-LLM layers. However, these require at least partial processing of the video, which can be expensive for larger models, and it is likely that the most informative features will be those of the later layers [55], at which point there is not much computational savings. The second is the use of approaches that ignore explainability, *i.e.* fail to define the vocabulary of video attributes that contribute to complexity and characterize complexity in terms of these attributes. To address this problems, we propose a *non-parametric* alternative based on the *explicit* characterization of complexity in terms of video attributes. We denote the approach as *Attribute-Based Complexity* (ABC) of video, or VideoABC.

VideoABC is a non-parametric complexity score that, as illustrated in Figure 1, is computed with respect to an external reference video dataset \mathcal{D} , as is usual for *retrieval-augmented* (RAG) architectures. Given a dataset \mathcal{D} of reference videos, a vocabulary of complexity attributes \mathcal{A} is first defined and procedures designed to extract or control the values of the video attributes in \mathcal{A} . Each video is then represented as a vector in an attribute vector space \mathcal{S}_A whose dimensions are the attributes of \mathcal{A} . The space is then quantized, to produce a codebook \mathcal{C} of representative attribute vectors, The expected ABC of each quantizer cell is then computed by processing its video-question pairs and

tallying successes and failures. Given an unseen video, the associated attribute vector is computed and quantized with \mathcal{C} , and the complexity score of the associated bin is returned.

VideoABC supports any attribute vocabulary \mathcal{A} . In this work, we use a vocabulary inspired by the historical evolution of video benchmarks. Early benchmarks [24, 44] typically consisted of short videos with relatively simple visual dynamics. As video understanding models improved, benchmarks increased the level of difficulty by introducing longer videos and more complex questions [30, 65, 61]. Over time, as models adapted to these challenges, benchmarks [36, 60, 33, 41] further raised difficulty by incorporating even longer videos, more visually complex frames, and faster or denser events. This progression suggests the importance of attributes like video length, event location, event speed, and frame complexity. We thus use these attributes as attribute vocabulary \mathcal{A} . While we do not claim that this vocabulary is exhaustive, our results show that it enables effective predictions of video complexity with low-dimensional attribute vectors.

The central technical component of VideoABC is the quantizer \mathcal{C} , which determines the balance of performance between in-distribution (ID) data (similar to \mathcal{D}) and out-of distribution (OOD) data (unrelated videos). In order to enable the deployment of VideoABC without massive reference datasets, we propose a combination of two quantizers. The first is an in-distribution quantizer, learned with by applying k-means to the attribute vectors extracted from \mathcal{D} . The second is a universal quantizer designed using synthetic videos with carefully controlled attribute values, so as to provide coverage of the entirety of the attribute space $\mathcal{S}_{\mathcal{A}}$. This is a lattice quantizer, where \mathcal{C} is implemented as $\mathcal{C} = \mathcal{C}_1 \times \dots \times \mathcal{C}_{|\mathcal{A}|}$ and \mathcal{C}_k is a scalar quantizer for attribute k . This enables the training of the quantizer one-attribute-at-a-time, using a dataset of synthetic video question pairs \mathcal{F}_k where only attribute k is varied. For this, we propose a procedure inspired by psychophysics studies of human attention [22, 52, 51, 49, 48, 47, 23, 50, 58, 8, 56, 57], based on the manipulation of a target object embedded into a video of distractor objects. This procedure is used to generate a dataset of synthetic video-question pairs conditioned on user-specified attribute values, so as to cover the entire range of values of each complexity attribute.

Experimental results show that VideoABC is significantly more effective at predicting the complexity of video-question pairs than various parametric approaches, including the popular use of an external video-LLM as judge. The gains are significant in terms of both the calibration of the complexity score and its computational efficiency. We also demonstrate how the explainable nature of a complexity score based on well-defined attributes provides insights on how the attribute composition of benchmarks affects their complexity, and the sensitivity of different models to different complexity attributes. In the supplement, we provide some preliminary examples of how VideoABC can be leveraged to implement effective curriculum learning and model distillation strategies.

Contributions. Our main contributions are as follows: 1) the VideoABC framework to quantify video-question complexity in terms of well defined video attributes, 2) a procedure for effective attribute quantizer design from small reference datasets using 3) a combination of k-means and lattice quantization, and 4) a procedure for the synthesis of videos with controllable attributes to allow lattice-based complexity estimation. We also present experiments illustrating of VideoABC can provide valuable insights about video benchmarks and applications.

2 Background

Video Attributes. The study of video attributes that affect model performance has a long history in computer vision. For example, early work in representation bias [30] identified the tendency of early video datasets (*e.g.* KTH [42], Weizmann [20], UCF101 [44], Kinetics [24]) to favor short-term video representations. This motivated the introduction of datasets, like Diving48 [30], MVBench [29], LongVideoBench [60], MLVU [65], ApoLLO [67], Cinepile [41], NextQA [61], TempCompass [33] to name a few, without this property and work on long-term video representations, which are now the focus of most video model design efforts [64, 63, 28, 31, 26]. More recently, some work in the literature has started to address the problem of characterizing the attributes of video complexity. For example, the benchmark of [36] comprehensively evaluates how video-LLM performance depends on event length. All these works tend to show that attributes are primary factors for affecting complexity in videos. Motivated by their insights, we propose a complexity score that depends only on these attributes.

Characterizing Complexity. Earlier video benchmarks, such as those introduced in [42, 20, 44], primarily evaluated video understanding models on short clips. Subsequent datasets incorporated more

visually complex scenes [24]. As more capable video-LLMs emerged [63, 62, 28, 31], the community sought to increase benchmark difficulty by curating short videos with rapidly evolving events [6, 25, 30], *i.e.* scenarios in which models must process a larger number of frames to answer correctly. With the advent of transformer-based architectures and, consequently, video-LLMs with substantially longer context windows [63, 28], this challenge was largely mitigated. More recent benchmarks [17, 65, 60, 36, 41, 29, 33, 61] now feature significantly longer videos, rapidly changing events, and a broader diversity of question types, moving beyond the earlier focus on action recognition [24, 30]. Notably, this progression reveals a consistent pattern in benchmark design: increasing difficulty by systematically modifying video attributes. The benchmarks have transitioned from short videos to visually complex scenes, then to fast-evolving events, and ultimately to substantially longer videos. Inspired by this trend of evolving benchmark curation, we propose to directly leverage these attribute dimensions as explicit dimensions of complexity.

3 The VideoABC framework

In this section, we introduce *Video Attribute Based Complexity* (VideoABC), a non-parametric framework for characterizing video complexity in terms of video attributes.

3.1 Complexity measure

VideoABC is a non-parametric measure of video-question pair complexity. Let $\mathbf{v} = [v_1, \dots, v_N] \in \mathbb{R}^{N \times H \times W \times 3}$ be a video with N RGB frames $v_k \in \mathbb{R}^{H \times W \times 3}$ of height H and width W . Given a video-LLM \mathcal{M} , the complexity posed by video-question pair (\mathbf{v}, q) to \mathcal{M} is a score $c \in [0, 1]$, reflecting the probability that \mathcal{M} will fail to solve q . Let $\mathcal{A} = \{a_1, \dots, a_D\}$ be a set of D video attributes and $\mathbf{a} = \alpha(\mathbf{v}, q)$ the embedding of (\mathbf{v}, q) in a unit D -cube $\mathcal{S}_{\mathcal{A}} = [0, 1]^D$ of attributes defined by \mathcal{A} . VideoABC computes a nonparametric measure of complexity $c = \gamma(\mathbf{a}, \mathcal{D})$ using a reference dataset $\mathcal{D} = \{(\mathbf{v}_i, q_i)\}_i$ of video question pairs, using the two-stage procedure of Figure 1.

In a training stage, \mathcal{D} is used to design a vector quantizer of $\mathcal{S}_{\mathcal{A}}$, consisting of a codebook \mathcal{C} with attribute templates $\{\mathbf{c}_j \in \mathcal{S}_{\mathcal{A}}\}_{j=1}^J$ and associated quantization rule,

$$\mathcal{Q}(\mathbf{a}; \mathcal{D}) = \arg \min_{j \in \{1, \dots, J\}} \|\mathbf{a} - \mathbf{c}_j\|, \quad (1)$$

which assigns \mathbf{a} to the nearest neighbor template. Each attribute vector \mathbf{a} in \mathcal{D} is then mapped by \mathcal{Q} into one of the quantizer cells

$$\mathcal{N}_j = \{\mathbf{a} \mid \|\mathbf{a} - \mathbf{c}_j\| \leq \|\mathbf{a} - \mathbf{c}_l\|, \forall l \neq j\}, j = \{1, \dots, J\}. \quad (2)$$

The model \mathcal{M} is then applied to each of the pairs $(\mathbf{v}_i, q_i) \in \mathcal{D}$ such that $\alpha(\mathbf{v}_i) \in \mathcal{N}_j$ and a binary function $y(\mathbf{v}, q)$ used to indicate success ($y = 1$) or failure ($y = 0$) in answering question q_i . The *Expected Attribute Based Complexity* (EABC) of cell \mathcal{N}_j is finally defined as the failure rate of the videos mapped to the cell,

$$\psi_j = 1 - \frac{1}{|\{i \mid \alpha(\mathbf{v}_i, q_i) \in \mathcal{N}_j\}|} \sum_{i \mid \alpha(\mathbf{v}_i, q_i) \in \mathcal{N}_j} y(\mathbf{v}_i, q_i). \quad (3)$$

This procedure produces a pair of attribute template and video complexity (\mathbf{c}_j, ψ_j) per cell \mathcal{N}_j .

At inference, the complexity of a video question pair (\mathbf{v}, q) is computed by quantizing \mathbf{v} with (1) and returning the associated cell EABC,

$$\gamma(\mathbf{v}, q; \mathcal{D}) = \psi_{\mathcal{Q}(\alpha(\mathbf{v}, q); \mathcal{D})}. \quad (4)$$

3.2 Codebook Design

The simplest strategy to design the codebook \mathcal{C} is to apply a clustering algorithm to the reference dataset \mathcal{D} . In this work, we rely on k-means [12]. However, the accuracy of the resulting complexity measure of (4) depends on the relationship between \mathbf{v} and \mathcal{D} , as illustrated in Figure 2. If (\mathbf{v}, q) is in-distribution, it will likely be mapped to a densely populated cell, leading to an accurate estimate. However, if (\mathbf{v}, q) is out of distribution, it could easily land on a large and sparsely populated cell. In this case, $\gamma(\mathbf{v}, q; \mathcal{D})$ can be a poor estimate of the real complexity. One strategy

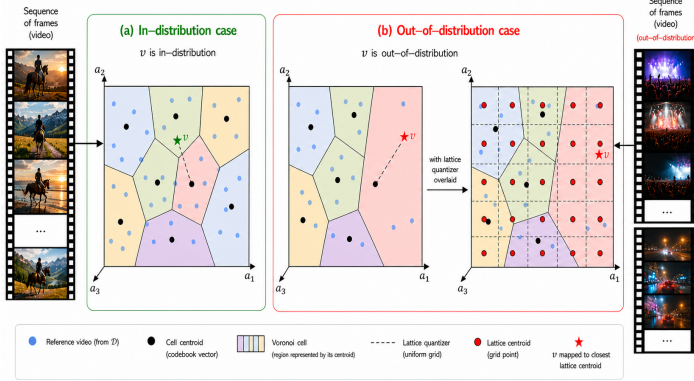


Figure 2: Left: a K-means quantizer \mathcal{C} is effective for videos similar to those of \mathcal{D} (in-distribution). Right: however, out-of distribution videos can land on large and sparsely populated cells, leading to poor ABC estimates. A universal lattice quantizer \mathcal{C}^u provides uniform coverage of the space, improving generalization.

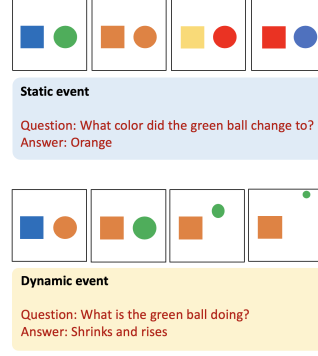


Figure 3: Examples of video-question pairs with static and dynamic events used to train the universal quantizer.

to address this problem is to rely on a very large \mathcal{D} . However, beyond the practical difficulties of learning with large datasets, it is difficult to know when \mathcal{D} covers the space \mathcal{S}_A well enough to avoid out-of-distributions problems. In this work, we consider the alternative of relying on a *universal codebook* \mathcal{C}^u , implemented with lattice quantization [9]. This consists of designing \mathcal{C}^u as a regular template grid, i.e. $\mathcal{C}^u = \mathcal{C}_1^u \times \dots \times \mathcal{C}_D^u$, where \mathcal{C}_k^u is a scalar quantizer of attribute a_k . Each dimension k of \mathcal{S}_A is divided into P uniform bins $\{\mathcal{B}_{k,j} = [b_{j-1} = \frac{j-1}{P}, b_j = \frac{j}{P}]\}_{j=1}^P$ of center point $c_{k,j} = \frac{2j-1}{2P}$, where the b_i are bin delimiters shared by all the D dimensions. This produces a total of P^D bins. The centers of these bins are used as templates of \mathcal{C}^u , i.e. $\mathbf{c}_j = [c_{1,j}, \dots, c_{P,j}]$.

While the use of this quantizer guarantees a uniform coverage of the attribute space by \mathcal{S}_A by the quantization cells \mathcal{N}_k , it makes the computation of the EABC of every cell difficult. Assume that C videos are required per cell, to produce an accurate estimate of the EABC. Then, the computation of (3) for cell \mathcal{N}_k requires a dataset of C videos with the combination of attribute values that make up the template attribute vector \mathbf{c}_k . However, identifying videos with this particular combination of attribute values in the wild is a ‘needle-in-the-haystack’ problem. To overcome this problem, we propose to use instead a reference dataset \mathcal{D}^u of synthetic video, which allows the generation of videos with attribute vector \mathbf{c}_k on demand. We then generate C videos per cell, process them with the target video-LLM, compute success/failures and use (3) to compute the cell EABC. This produces the set of EABCs ψ_j^u associated with the templates \mathbf{c}_j of the universal quantizer \mathcal{C}^u .

However, even this procedure can be too complex, since it requires the generation of $C \times P^D$ videos and their processing by the target video-LLM. As the dimension D of the attribute embedding increases, the computation becomes unfeasible. We address this problem by learning attribute complexities independently. For each scalar quantizer \mathcal{C}_k^u of \mathcal{C}^u , we use the video generation procedure to generate C videos per quantization bin of the values of attribute a_k . We then compute the bin EABC using an attribute specific version of (3)

$$\psi_{k,j}^u = 1 - \frac{1}{|\{i | \alpha_k(\mathbf{v}_i, q_i) \in \mathcal{B}_{k,j}\}|} \sum_{i | \alpha_k(\mathbf{v}_i, q_i) \in \mathcal{B}_{k,j}} y(\mathbf{v}_i, q_i). \quad (5)$$

where $\mathcal{B}_{k,j}$ is the j^{th} bin of the quantizer \mathcal{C}_k^u of the k^{th} attribute $\alpha_k(\mathbf{v}, q)$ of pair (\mathbf{v}, q) and $\psi_{k,j}^u$ the associated EABC. This only requires the generation of $P \times D$ videos and the computation of $P \times D$ EABCs. Finally, for each cell \mathcal{N} of \mathcal{C}^u , we find the corresponding bins $\mathcal{B}_{k,j(\mathcal{N})}$ for each attribute dimension k , and approximate the cell EABC by the largest of the bin EABCs,

$$\hat{\psi}^u(\mathcal{N}) = \max_k \psi_{k,j(\mathcal{N})}^u. \quad (6)$$

This assumes that attributes have a disjunctive (logical OR) relation, e.g. a video can be complex because the event of interest is fast *or* the scene is complex. This procedure produces a set of approximate EABCs $\hat{\psi}_j^u$ associated with the templates \mathbf{c}_j of the universal quantizer \mathcal{C}^u .

3.3 Video Attributes

The aim of this work is not to produce an exhaustive list of all attributes that affect video complexity. While VideoABC is applicable to any choice of \mathcal{A} , we focus on a small set of *event-based* attributes. An *event* $\mathcal{E}(q) \subseteq \mathcal{V}$ is a video clip informative of a question q . Let $\mathcal{E}(q) = [e_1, \dots, e_{N_E}]$ be an event of $N_E \leq N$ frames, where $e_k = v_{j+k-1}$, $k \in \{1, \dots, N_E\}$. We consider six attributes. Attribute a_1 is the **event location**, i.e. $a_1 := j$. The complement of $\mathcal{E}(q)$ in \mathbf{v} , i.e. $\bar{\mathcal{E}}(q) = \mathbf{v} \setminus \mathcal{E}(q)$, is denoted as the *non-event* video. Attribute a_2 is the **non-event proportion**, $a_2 := 1 - |\bar{\mathcal{E}}(q)|/N$. Attribute a_3 , denoted as **scene complexity**, is the number of objects unrelated to the event present in the video. We provide below more details on how this number is determined. Finally, attribute a_4 is the **event speed**. This is the smallest frame rate f^1 at which the video-LMM correctly answers question q from the resampled video, i.e. $a_4 := \arg \min_{\rho} \mathbb{1}[u(\mathbf{v}^\rho, q) = 1]$, where \mathbf{v}^ρ is the video resampled at frame rate ρ , and $u(\mathbf{v}, q) = 1$ if q is correctly answered for \mathbf{v} and 0 otherwise. These four attributes were chosen because they have been previously hypothesized to affect complexity by the video understanding community. For instance, non-event proportion and scene complexity have been previously leveraged to curate hard benchmarks in [29, 60, 65, 41]. Similarly, event speed has been utilized in benchmarks like [30, 65, 29]. To test the robustness of VideoABC to the inclusion in \mathcal{A} of attributes uninformative of video complexity we also considered two such attributes. Attribute a_5 is the **ratio between median and maximum pixel values** in the video i.e. $a_5 := \text{median}(\mathbf{v})/\text{max}(\mathbf{v})$. Attribute a_6 is the **ratio between mean and maximum pixel values** i.e. $a_6 := \text{mean}(\mathbf{v})/\text{max}(\mathbf{v})$.

3.4 Datasets and Complexity Measures

In-distribution quantizer. To train the in-distribution quantizer \mathcal{C} , we use a reference dataset \mathcal{D} of 300 videos from each of four SOTA benchmarks: MV-Bench [29], MLVU [65], TempCompass [33] and NextQA [61]. The resulting dataset has 1200 real video-question pairs. To measure attribute values of video-question pair (\mathbf{v}, q) , we define the event informative of the question as

$$\hat{\mathcal{E}}(q) = \arg \max_{\mathcal{E} \subseteq \mathbf{v}, |\mathcal{E}|=K} S(\mathbf{v}; q) \quad (7)$$

where K is a target event clip size and S a question-relevance score implemented with the *DINO score* of [19] per video frame and summing over \mathcal{E} . Given $\hat{\mathcal{E}}(q)$, the values of all attributes other than a_3 follow trivially from the attribute definitions above. To estimate the scene complexity attribute a_3 , we computed its average compression ratio i.e. $a_3 := \frac{1}{K} \sum_{i=1}^K c_i$ where c_i is the compression ratio of frame i . This procedure generates a dataset of 1200 6-dimensional attribute vectors, to which k-means [12] is applied to assign these attribute vectors to the cells of quantizer \mathcal{C} . The EABC of each quantizer cell is finally estimated with (3).

Universal quantizer. As discussed above, the design of \mathcal{C}^u is based on a dataset of synthetic videos that allows the manipulation of attribute values one-at-a-time. In this case, since the attribute values are known for all videos, there is no need for a procedure to estimate attribute values. To generate synthetic videos with specified attribute values, we propose a procedure inspired by the psychophysics literature [15, 10, 18, 37, 13, 5, 34, 53], using 1) videos such as those shown in Figure 3 and 2) the target-distractor manipulations popular in studies of human attention [59]. Every video uses a green ball as target object, the video-LLM is asked a question q grounded on an event $\mathcal{E}(q)$, and presented with 5 answers. Events are defined by the change of a single target property, e.g. color in Figure 3 (top). Two types of events are defined².

1. **Static events.** Manipulations change a static target property. As shown in Figure 3 (top), event \mathcal{E} is a color change of the green ball at a unique *event location* (frame pair) in the video. The task is to choose from one of five possible locations.
2. **Dynamic events.** Manipulations are dynamic, namely the combination of (upward or downward) ball motion and variation (increase or decrease) of ball size. Figure 3 (bottom) shows an example where the ball moves up and shrinks. The task is to choose from one of the four possible combinations of motion and shape change plus ‘none of the above’.

The remaining balls and squares in the video are distractors chosen randomly (restricting ball colors to non-green) per frame pair. The number of these objects is the scene complexity attribute a_3 .

¹The frame rate of \mathcal{V} is $\rho = \frac{N}{T}$, where T is the temporal duration of \mathcal{V} in seconds.

²More details about the dataset curation are provided in appendix C.

Static events are used to quantify video complexity as a function event position (a_1), non-event proportion (a_2) and ratios (a_5 and a_6). Dynamic events are used to quantify complexity as a function of scene complexity (a_3) and event speed (a_4). To learn approximate EABCs, for each attribute a_k and attribute bin $\mathcal{B}_{k,j}$, we generate C synthetic video-question pairs and use (5) to estimate the bin EABC. The total number of samples needed to cover the P attribute bins of each scalar quantizer \mathcal{C}_k^u is $C \times P$. Given all individual attribute EABCs, we use (6) to compute the approximate EABC $\hat{\psi}_j^u$ of each cell \mathcal{N}_j of \mathcal{C}^u . The overall dataset \mathcal{D}^u needed to learn all EABCs has size $C \times P \times D$. It is also possible to learn exact EABCs, by generating C videos with the attribute combination c_k of each of the P^D bins \mathcal{N}_k of \mathcal{C}^u and using (3) to compute the corresponding EABC ψ_k^u . This requires $C \times P^D$ videos.

Combined quantizer. As discussed above, the two quantizers have different weaknesses. The in-distribution quantizer \mathcal{C} cannot finely cover the entire vector space \mathcal{S}_A . Hence, it generalizes poorly to videos outside the distribution of \mathcal{D} . The universal quantizer \mathcal{C}^u eliminates this problem, but provides a weaker EABC estimate for in-distribution videos, due to both the reliance on lattice quantization and the approximation of (5). This suggests combining the two quantizers, using \mathcal{C} for videos in the distribution of \mathcal{D} and \mathcal{C}^u for out-of-distribution videos. For this, we propose the following simple rule

$$\gamma(\mathbf{v}, q; \mathcal{D}) = \begin{cases} \psi(\mathcal{N}_j) & \text{if } \exists c_j \in \mathcal{C} \text{ s.t. } \|\alpha(\mathbf{v}, q) - c_j\|_2^2 \leq \tau \\ \psi^u(\mathcal{N}_j) & \text{otherwise.} \end{cases}$$

This reflects the intuition that if the attribute vector of (\mathbf{v}, q) is too far from the closest template of the in-distribution quantizer \mathcal{C} , then we rely on the out-of-distribution quantizer. Otherwise, we rely on in-distribution quantizer. The threshold τ chosen is 2.4 and is obtained by cross-validation.

Computational cost. VideoABC is extremely efficient at inference, since the extraction of the attribute vector $\alpha(\mathbf{v}, q)$ and the quantization operations required by either (3) or (5) use orders of magnitude less computation than computing video-LLM features for \mathbf{v} . The main computational cost is in quantizer design during the training stage. This requires performing video-LLM inference on all videos of \mathcal{D} or \mathcal{D}^u , in order to compute (3) or (5), respectively, for each quantizer cell. This cost depends on the quantizer, as discussed above, ranging from $\mathcal{O}(CP)$ for the in-distribution quantizer to $\mathcal{O}(CP^D)$ for the universal quantizer with exact EABCs.

4 Experiments

In this section, we report on various experiments performed to evaluate the VideoABC framework.

Implementation details. We considered 5 SOTA video-LLMs of different sizes – Qwen-3.5-VL (4B, 9B) [63], LLaVA-OV (0.5B, 7B) [28], LLaVA-NeXT (7B) [64] and Video-LLaVA (7B) [31]. Due to space constraints, we present results for 5 models in the paper and the remaining in supplementary. Models were used with default parameters and initialized from Huggingface. 4×NVIDIA-A6000 GPUs were used for implementation. All code and datasets will be shared upon paper publication.

Metrics. Since the EACB is an estimate of the probability of video-LLM failure, we rely on the Expected Calibration Error (ECE) [4, 38] to test the effectiveness of VideoABC. This metric is commonly used to evaluate the calibration of probability estimates [38, 3, 11].

Baselines. Unfortunately, most complexity scores used in the recent literature [40, 45, 14, 21] are closed-sourced, making direct comparisons impossible. Instead, we compare VideoABC to several baselines of comparable architecture. The primary baseline is the popular **video-LLM-as-judge** method (denoted Judge), where an external video-LLM is asked to estimate the complexity of the video-question pair (\mathbf{v}, q) . This approach is widely used in the literature [14, 21, 2]. In our experiments, we use Qwen-3.5-VL (7B and 72B) models as external judge, unless otherwise specified. Note that when the target video-LLM is one of these models the approach is internal. The second baseline, denoted as MLP-2L, is an internal method. It uses a **2-layer MLP** to predict complexity from a feature vector extracted at the input of the penultimate layer embedding of the target video-LLM. The MLP is a binary classifier, trained to predict the target video-LLM failures ($y = 0$) and successes ($y = 1$). The third baseline, denoted as Direct, bypasses the computation of the EABC. We simply extract the attribute vector from (\mathbf{v}, q) and use the attribute values directly to create a complexity score. Similarly to (6) we use the maximum attribute value $\max(\alpha(\mathbf{v}, q))$ as complexity measure. The fourth baseline, denoted as MLP-A, is an attribute **MLP classifier**, which maps attribute values

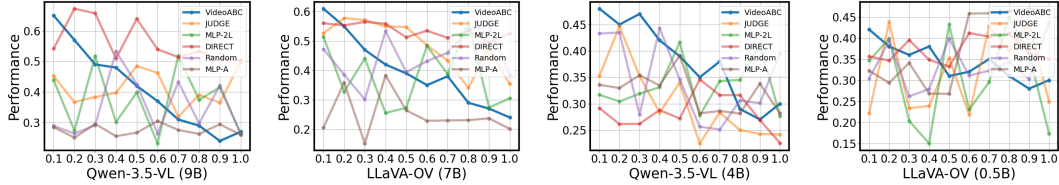


Figure 4: Video-LLM performance p as a function of complexity score γ for models of different sizes.

Video-LLM	Random	Judge	Direct	MLP-2L	MLP-A	VideoABC
Large size						
Qwen-3.5-VL _(9B)	0.293	0.171	0.194	0.217	0.197	0.087
LLaVA-OV _(7B)	0.328	0.148	0.200	0.285	0.156	0.058
Video-LLaVA _{7B}	0.346	0.173	0.189	0.292	0.192	0.097
LLaVA-Next _{7B}	0.329	0.121	0.203	0.308	0.146	0.102
Small size						
Qwen-3.5-VL _{4B}	0.348	0.208	0.246	0.322	0.198	0.156
LLaVA-OV _{0.5B}	0.348	0.198	0.256	0.347	0.234	0.172

Table 1: Comparison of the ECE (\downarrow) of VideoABC and baselines for several target video-LLMs. LLaVA-OV (7B) was used as Judge.

Method	Size	Time (ms)	Performance
Judge	0.5B	167	0.187
	3B	427	0.187
	7B	656	0.171
	72B	1802	<u>0.164</u>
Direct	-	201	0.194
MLP-2L	9B	678	0.217
MLP-A	-	119	0.182
Random	-	10	0.293
VideoABC	-	226	0.087

Table 2: Comparison of model size, inference latency and ECE (\downarrow).

to target video-LLM success/failures. The final baseline, denoted as **Random**, is a **random score generator** that uniformly samples a number in $[0, 1]$.

Evaluation datasets. VideoABC is evaluated on two datasets. The first is an in-domain (Eval-ID) dataset, composed of 1200 videos samples from the four datasets used to curate the reference dataset \mathcal{D} on which the in-distribution quantizer \mathcal{C} is trained. The second is an out-of-domain (Eval-OOD) dataset composed of 1200 videos from Egoschema [36] and LongVideoBench [60]. The OOD dataset is used for all experiments unless otherwise stated.

4.1 Results.

In this section, we present the major results characterizing the performance of VideoABC. Detailed ablations of model parameters are presented in the supplement.

Qualitative results. We start with a qualitative comparison between VideoABC and baselines in Figure 4. The figures show plots of video-LLM performance p as a function of the video-question complexity score γ , for several video-LLMs. To produce these plots, we quantized the complexity score into ten bins and present the success rate per bin. The ideal plot would be a curve of the form $p = 1 - \gamma$ that also accounts for the fact that p saturates and never reaches 0 nor 1. We did not attempt to compress or normalize the complexity scores to reflect this. The plots of VideoABC are much closer to ideal than those of all baselines. Most baseline curves lack the monotonically decreasing and almost linear trend of VideoABC. The figure also shows that the difficulty of complexity predicting is harder for the smaller models on the right. Beyond the compression of performance range, due to the lower model capacity that upper bounds the plots, most curves have higher p values for the highest complexity ($\gamma = 1$), suggesting that some easier video-question pairs receive high complexity scores.

Quantitative results. Table 1 compares the ECE of the different methods for all six models. VideoABC achieves significantly lower ECE than all baselines, indicating stronger calibration with video-LLM performance, for all models. Among the baselines, Judge achieves the best performance. The internal MLP-2L method has surprisingly weak performance, showing that it may not be easy to extract signals predictive of success/failure from the target video-LLM itself. This is consistent with the well known difficulties of detecting LLM hallucinations [32, 46]. The improved performance of Direct shows that video attributes are much more informative of video complexity and that the disjunctive assumption behind (6) preserves much of that information. In fact, for the larger models Direct approaches the performance of Judge. MLP-A has similar but more variable performance. This is due to poor generalization of the MLP trained on a small set of real videos attribute vectors (only 1200). A more robust MLP would require a larger sample size and would significantly increase computational cost. Nevertheless, its gains over Direct for some target video-LLMs show that the disjunctive assumption of (6) can incur losses. In conclusion, these results demonstrate that video attributes are reliable predictors of video-question complexity and that VideoABC produces significantly more reliable and efficient complexity estimates than existing baselines.

VideoABC	Templates	Eval-00D						Eval-ID					
		\mathcal{M}_1	\mathcal{M}_2	\mathcal{M}_3	\mathcal{M}_4	\mathcal{M}_5	\mathcal{M}_6	\mathcal{M}_1	\mathcal{M}_2	\mathcal{M}_3	\mathcal{M}_4	\mathcal{M}_5	\mathcal{M}_6
(\mathcal{C}, ψ)	20	0.114	0.117	0.097	0.097	0.092	0.089	0.069	<u>0.062</u>	<u>0.087</u>	0.085	<u>0.074</u>	<u>0.072</u>
$(\mathcal{C}^u, \hat{\psi}^u)$	180	<u>0.082</u>	0.062	<u>0.058</u>	0.082	<u>0.067</u>	<u>0.059</u>	0.095	0.088	0.104	0.096	0.092	0.092
(\mathcal{C}^u, ψ^u)	10000	0.076	0.052	0.054	<u>0.087</u>	0.066	0.059	<u>0.085</u>	0.056	0.082	<u>0.087</u>	0.068	0.068
$(\mathcal{C}, \psi) \cup (\mathcal{C}^u, \hat{\psi}^u)$	200	0.087	<u>0.058</u>	0.054	0.082	0.064	0.059	<u>0.072</u>	0.054	0.094	0.096	0.087	0.084

Table 3: ECE and number of template computations for different EABC estimation strategies on the Eval-00D and Eval-ID datasets. **Bold letters** denote best performance while underlined letters denote second best performance. \mathcal{M} denotes different video-LLMs in order described in implementation details (sec 4)

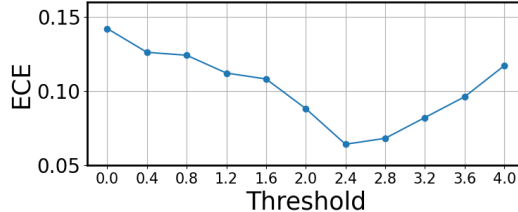


Figure 5: Figure show how ECE varies with respect to threshold of combined quantizer.

Inference Latency. Table 2 compares the computational requirements of VideoABC and baselines³. VideoABC is approximately 8 times faster than a 72B Judge and has latency comparable to a 0.5B Judge. On the other hand, VideoABC substantially outperforms both the 72B and 0.5B Judge models. In other words, VideoABC matches the efficiency of a 0.5B Judge while outperforming even a 72B Judge. It also has no significant memory requirements. The latency of VideoABC is comparable to most other baselines, which VideoABC again outperforms substantially. The approaches with the next best trade-offs between complexity and performance are MLP-A and Direct, again showing the benefits of ABC predictions.

Robustness. To test the robustness of VideoABC to attribute noise, we included in \mathcal{A} non-informative attributes a_5, a_6 , which are expected not to affect video-LLM performance. We performed a linear regression with attribute values as inputs and VideoABC scores as output. The magnitude of the weight learned per attribute measures its importance to the regression. Figure 7 shows these weights. The contributions of a_5 and a_6 are minimal compared to those of the remaining attributes. This shows that VideoABC can effectively ignore non-informative attributes.

4.2 Ablation

In this section, we discuss various ablations of VideoABC.

Codebook. Table 3 compares variants of VideoABC with different quantizer and EABC computations: in-distribution quantizer \mathcal{C} , universal quantizer \mathcal{C}^u with approximate EABC $\hat{\psi}^u$ or true EABC ψ^u and combined quantizer $(\mathcal{C}, \psi) \cup (\mathcal{C}^u, \hat{\psi}^u)$. Several observations can be made. First, while the in-distribution quantizer (\mathcal{C}, ψ) outperforms the approximate universal quantizer $(\mathcal{C}^u, \hat{\psi}^u)$ for in-domain evaluation (Eval-ID), the latter has significantly better performance in the out-of-domain setting (Eval-00D). This confirms that, while k-means is more effective for in-distribution data, lattice quantization guarantees better generalization. Second, while the universal quantizer with exact EABC (\mathcal{C}^u, ψ^u) has the overall best performance, it requires a large number of bins. This drastically increases the computation and storage needed to create videos, process them with the target video-LLM, and store them. However, it only slightly outperforms the combined quantizer $(\mathcal{C}, \psi) \cup (\mathcal{C}^u, \hat{\psi}^u)$, which requires orders of magnitude less bins. Overall, the combined quantizer achieves the best trade-off between performance and training complexity. In fact, the implementation of VideoABC with the combined quantizer is close to the best performance for both the in-distribution and out-of-distribution settings, for all video-LLMs. We thus use this configuration in all experiments.

Codebook size. The sizes of both codebooks were varied in the experiments. Figure 6 presents the results for the two codebooks across different sizes. Both in-distribution quantizer and universal quantizer was tested on concatenated Eval-ID and Eval-00D datasets. Two key conclusions emerge. First, varying J in the in-distribution quantizer has little effect on performance beyond a certain point; in our experiments, this threshold was around 20. Beyond this value, there is no significant

³We exclude the training time required to construct the VideoABC codebook.

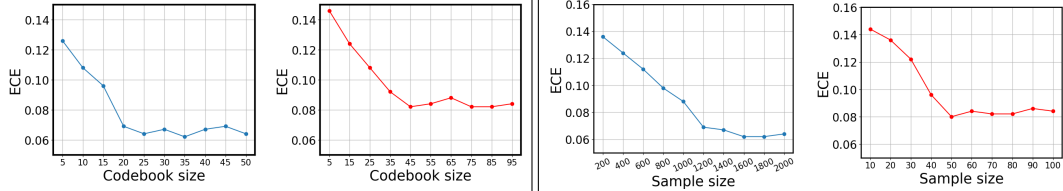


Figure 6: Left: ECE (\downarrow) vs codebook size for in-distribution (blue) and universal (red) quantizers. Right: ECE (\downarrow) vs sample size for in-distribution (blue) and universal (red) quantizers. The in-distribution and universal quantizers were tested on Eval-ID and Eval-ODD datasets respectively.

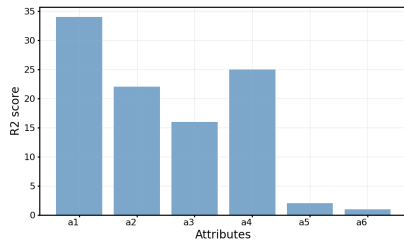


Figure 7: Attribute weights of VideoABC score regression.

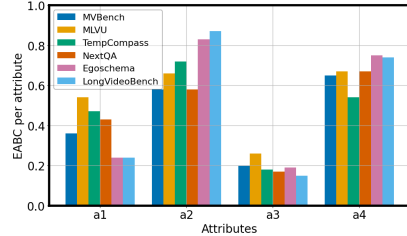


Figure 8: Average attribute EABC for different benchmarks. Attributes a5 and a6 are omitted, due to their minimal contribution to video complexity.

improvement in the model’s ECE. Second, for the universal quantizer, increasing P leads to improved performance initially, but gains diminish after an upper threshold, where performance begins to plateau. Overall, for both quantizers, performance improves with increasing values of J and P at lower ranges, followed by saturation.

Sample size. Figure 6 (right) shows the effect of sample size on VideoABC performance. For the in-distribution quantizer \mathcal{C} , sample size is the size of the reference dataset $|D|$. For the universal quantizer \mathcal{C}^u , it is the number of videos synthesized per attribute to estimate the per-attribute complexity of (5). One can note that as the total number of real videos increases, the computational complexity of the in-distribution quantizer gradually saturates to a fixed value. For the universal quantizer, performance improves as the sample size *per bin* increases. For real videos, we report results in terms of total samples, whereas for synthetic data we report per-bin sample sizes. This distinction arises because controlling the number of samples per bin is straightforward in the synthetic setting, while for in-distribution data it is significantly more difficult, as it depends heavily on the available dataset. Our experiments further show that randomly sampling videos from diverse datasets effectively alleviates this limitation and yields stable performance.

Threshold of combined quantizer. We ablated the threshold of the combined quantizer, (τ), on a concatenated Eval-ODD and Eval-ID dataset. The results are shown in figure 5. As the threshold distance increases, performance initially declines slightly and then drops sharply. This behavior arises because predictions are increasingly dominated by the in-distribution quantizer, which is not well-suited for handling Eval-ODD samples. Conversely, when the threshold is reduced, most predictions are made by the universal quantizer; due to its approximate nature, its overall performance is also suboptimal. Notably, the performance degradation across threshold values is relatively modest, indicating that VideoABC is robust and does not degrade abruptly with changes in (τ).

Applications of VideoABC is presented in Appendix.

5 Discussion

Conclusion. We have introduced VideoABC, a framework for characterizing video-LLM complexity with respect to a pre-defined attribute vocabulary. VideoABC is a non-parametric complexity measure, based on the quantization of the attribute space and a reference dataset combining real and synthetic videos. Experiments have shown that it produces complexity estimates significantly better calibrated than those of various baselines, including the popular Judge approach, with much less complexity. A preliminary analysis of the attribute complexity of several benchmarks illustrates the potential of the measure for benchmark characterization.

References

- [1] Achiam, J., Adler, S., Agarwal, S., Ahmad, L., Akkaya, I., Aleman, F.L., Almeida, D., Altenschmidt, J., Altman, S., Anadkat, S., et al.: Gpt-4 technical report. arXiv preprint arXiv:2303.08774 (2023)
- [2] Agarwal, S., Krueger, G., Clark, J., Radford, A., Kim, J.W., Brundage, M.: Evaluating clip: towards characterization of broader capabilities and downstream implications. arXiv preprint arXiv:2108.02818 (2021)
- [3] Bella, A., Ferri, C., Hernández-Orallo, J., Ramírez-Quintana, M.J.: Calibration of machine learning models. In: Handbook of research on machine learning applications and trends: Algorithms, methods, and techniques, pp. 128–146. IGI Global Scientific Publishing (2010)
- [4] Böken, B.: On the appropriateness of platt scaling in classifier calibration. *Information Systems* **95**, 101641 (2021)
- [5] Broadbent, D.E.: Perception and communication. Elsevier (2013)
- [6] Caba Heilbron, F., Escorcia, V., Ghanem, B., Carlos Niebles, J.: Activitynet: A large-scale video benchmark for human activity understanding. In: Proceedings of the IEEE conference on computer vision and pattern recognition. pp. 961–970 (2015)
- [7] Chen, G., Zheng, Y.D., Wang, J., Xu, J., Huang, Y., Pan, J., Wang, Y., Wang, Y., Qiao, Y., Lu, T., et al.: Videollm: Modeling video sequence with large language models. arXiv preprint arXiv:2305.13292 (2023)
- [8] Chun, M.M., Wolfe, J.M.: Just say no: How are visual searches terminated when there is no target present? *Cognitive psychology* **30**(1), 39–78 (1996)
- [9] Conway, J.H., Sloane, N.J.A.: Sphere Packings, Lattices and Groups. Springer New York (1999)
- [10] Craik, F.I.: Effects of distraction on memory and cognition: a commentary. *Frontiers in psychology* **5**, 841 (2014)
- [11] Dormann, C.F.: Calibration of probability predictions from machine-learning and statistical models. *Global ecology and biogeography* **29**(4), 760–765 (2020)
- [12] Duda, R.O., Hart, P.E., Stork, D.G.: Pattern Classification (2nd Edition). Wiley-Interscience, 2 edn. (November 2000)
- [13] Ebbinghaus, H.: Über das gedächtnis: untersuchungen zur experimentellen psychologie. Duncker & Humblot (1885)
- [14] Eyzaguirre, C., Vasiljevic, I., Dave, A., Wu, J., Ambrus, R.A., Kollar, T., Niebles, J.C., Tokmakov, P.: Understanding complexity in videoqa via visual program generation. arXiv preprint arXiv:2505.13429 (2025)
- [15] Fechner, G.T.: Elemente der psychophysik, vol. 2. Breitkopf u. Härtel (1860)
- [16] Feng, B., Lai, Z., Li, S., Wang, Z., Wang, S., Huang, P., Cao, M.: Breaking down video llm benchmarks: Knowledge, spatial perception, or true temporal understanding? arXiv preprint arXiv:2505.14321 (2025)
- [17] Fu, C., Dai, Y., Luo, Y., Li, L., Ren, S., Zhang, R., Wang, Z., Zhou, C., Shen, Y., Zhang, M., et al.: Video-mme: The first-ever comprehensive evaluation benchmark of multi-modal llms in video analysis. In: Proceedings of the Computer Vision and Pattern Recognition Conference. pp. 24108–24118 (2025)
- [18] Geng, J.J.: Attentional mechanisms of distractor suppression. *Current Directions in Psychological Science* **23**(2), 147–153 (2014)
- [19] Goldstein, E.B.: Cognitive psychology: Connecting mind, research, and everyday experience. Cengage learning Stamford, CT (2015)
- [20] Gorelick, L., Blank, M., Shechtman, E., Irani, M., Basri, R.: Actions as space-time shapes. *IEEE transactions on pattern analysis and machine intelligence* **29**(12), 2247–2253 (2007)
- [21] Graves, A.: Adaptive computation time for recurrent neural networks. arXiv preprint arXiv:1603.08983 (2016)
- [22] James, W., Burkhardt, F., Bowers, F., Skrupskelis, K.: The principles of psychology. Macmillan London (1890)
- [23] Kahneman, D., Treisman, A., Gibbs, B.J.: The reviewing of object files: Object-specific integration of information. *Cognitive psychology* **24**(2), 175–219 (1992)
- [24] Kay, W., Carreira, J., Simonyan, K., Zhang, B., Hillier, C., Vijayanarasimhan, S., Viola, F., Green, T., Back, T., Natsev, P., et al.: The kinetics human action video dataset. arXiv preprint arXiv:1705.06950 (2017)
- [25] Kuehne, H., Jhuang, H., Garrote, E., Poggio, T., Serre, T.: Hmdb: a large video database for human motion recognition. In: 2011 International conference on computer vision. pp. 2556–2563. IEEE (2011)

- [26] Laurençon, H., Tronchon, L., Cord, M., Sanh, V.: What matters when building vision-language models? *Advances in Neural Information Processing Systems* **37**, 87874–87907 (2024)
- [27] Lavie, N.: Attention, distraction, and cognitive control under load. *Current directions in psychological science* **19**(3), 143–148 (2010)
- [28] Li, B., Zhang, Y., Guo, D., Zhang, R., Li, F., Zhang, H., Zhang, K., Zhang, P., Li, Y., Liu, Z., et al.: Llava-onevision: Easy visual task transfer. *arXiv preprint arXiv:2408.03326* (2024)
- [29] Li, K., Wang, Y., He, Y., Li, Y., Wang, Y., Liu, Y., Wang, Z., Xu, J., Chen, G., Luo, P., et al.: Mvbench: A comprehensive multi-modal video understanding benchmark. In: *Proceedings of the IEEE/CVF Conference on Computer Vision and Pattern Recognition*. pp. 22195–22206 (2024)
- [30] Li, Y., Li, Y., Vasconcelos, N.: Resound: Towards action recognition without representation bias. In: *Proceedings of the European conference on computer vision (ECCV)*. pp. 513–528 (2018)
- [31] Lin, B., Ye, Y., Zhu, B., Cui, J., Ning, M., Jin, P., Yuan, L.: Video-llava: Learning united visual representation by alignment before projection. In: *Proceedings of the 2024 Conference on Empirical Methods in Natural Language Processing*. pp. 5971–5984 (2024)
- [32] Liu, F., Liu, Y., Shi, L., Huang, H., Wang, R., Yang, Z., Zhang, L., Li, Z., Ma, Y.: Exploring and evaluating hallucinations in llm-powered code generation. *arXiv e-prints pp. arXiv-2404* (2024)
- [33] Liu, Y., Li, S., Liu, Y., Wang, Y., Ren, S., Li, L., Chen, S., Sun, X., Hou, L.: Tempcompass: Do video llms really understand videos? *arXiv preprint arXiv:2403.00476* (2024)
- [34] Loftus, E.F., Palmer, J.C.: Reconstruction of automobile destruction: An example of the interaction between language and memory. *Journal of verbal learning and verbal behavior* **13**(5), 585–589 (1974)
- [35] Lorenc, E.S., Mallett, R., Lewis-Peacock, J.A.: Distraction in visual working memory: Resistance is not futile. *Trends in cognitive sciences* **25**(3), 228–239 (2021)
- [36] Mangalam, K., Akshulakov, R., Malik, J.: Egoschema: A diagnostic benchmark for very long-form video language understanding. *Advances in Neural Information Processing Systems* **36**, 46212–46244 (2023)
- [37] Miller, G.A.: The magical number seven, plus or minus two: Some limits on our capacity for processing information. *Psychological review* **63**(2), 81 (1956)
- [38] Nixon, J., Dusenberry, M.W., Zhang, L., Jerfel, G., Tran, D.: Measuring calibration in deep learning. In: *CVPR workshops. vol. 2* (2019)
- [39] Pichai, S., Hassabis, D., Kavukcuoglu, K.: A new era of intelligence with gemini 3. Google. URL: <https://blog.google/products-and-platforms/products/gemini/gemini-3/> (2025)
- [40] Platanios, E.A., Stretcu, O., Neubig, G., Poczos, B., Mitchell, T.: Competence-based curriculum learning for neural machine translation. In: *Proceedings of the 2019 conference of the North American chapter of the association for computational linguistics: human language technologies, volume 1 (long and short papers)*. pp. 1162–1172 (2019)
- [41] Rawal, R., Saifullah, K., Farré, M., Basri, R., Jacobs, D., Somepalli, G., Goldstein, T.: Cinepile: A long video question answering dataset and benchmark. *arXiv preprint arXiv:2405.08813* (2024)
- [42] Schuldt, C., Laptev, I., Caputo, B.: Recognizing human actions: a local svm approach. In: *Proceedings of the 17th International Conference on Pattern Recognition, 2004. ICPR 2004. vol. 3*, pp. 32–36. IEEE (2004)
- [43] Smith, D.H., Poulsen, S., Emeka, C., Wu, Z., Haynes-Magyar, C., Zilles, C.: Distractors make you pay attention: Investigating the learning outcomes of including distractor blocks in parsons problems. In: *Proceedings of the 2024 ACM Conference on International Computing Education Research-Volume 1*. pp. 177–191 (2024)
- [44] Soomro, K., Zamir, A.R., Shah, M.: Ucf101: A dataset of 101 human actions classes from videos in the wild. *arXiv preprint arXiv:1212.0402* (2012)
- [45] Spitkovsky, V.I., Alshawi, H., Jurafsky, D.: Baby steps: How “less is more” in unsupervised dependency parsing. *NIPS: Grammar Induction, Representation of Language and Language Learning* pp. 1–10 (2009)
- [46] Sriramanan, G., Bharti, S., Sadasivan, V.S., Saha, S., Kattakinda, P., Feizi, S.: Llm-check: Investigating detection of hallucinations in large language models. *Advances in Neural Information Processing Systems* **37**, 34188–34216 (2024)
- [47] Treisman, A.: Search, similarity, and integration of features between and within dimensions. *Journal of Experimental Psychology: Human Perception and Performance* **17**(3), 652 (1991)
- [48] Treisman, A., Schmidt, H.: Illusory conjunctions in the perception of objects. *Cognitive psychology* **14**(1), 107–141 (1982)
- [49] Treisman, A., et al.: Features and objects in visual processing. *Scientific American* **255**(5), 114–125 (1986)

- [50] Treisman, A.M.: Contextual cues in selective listening. *Quarterly Journal of Experimental Psychology* **12**(4), 242–248 (1960)
- [51] Treisman, A.M.: Strategies and models of selective attention. *Psychological review* **76**(3), 282 (1969)
- [52] Treisman, A.M., Gelade, G.: A feature-integration theory of attention. *Cognitive psychology* **12**(1), 97–136 (1980)
- [53] Tversky, A., Kahneman, D.: Judgment under uncertainty: Heuristics and biases: Biases in judgments reveal some heuristics of thinking under uncertainty. *science* **185**(4157), 1124–1131 (1974)
- [54] Wang, C.: The dual system model of distraction: explaining the cognitive mechanism of distraction. *Frontiers in Psychology* **16**, 1632165 (2025)
- [55] Wiegrefe, S., Tafjord, O., Belinkov, Y., Hajishirzi, H., Sabharwal, A.: Answer, assemble, ace: Understanding how lms answer multiple choice questions. *arXiv preprint arXiv:2407.15018* (2024)
- [56] Wolfe, J.M.: Guided search 2.0 a revised model of visual search. *Psychonomic bulletin & review* **1**(2), 202–238 (1994)
- [57] Wolfe, J.M.: What can 1 million trials tell us about visual search? *Psychological Science* **9**(1), 33–39 (1998)
- [58] Wolfe, J.M., Cave, K.R., Franzel, S.L.: Guided search: an alternative to the feature integration model for visual search. *Journal of Experimental Psychology: Human perception and performance* **15**(3), 419 (1989)
- [59] Wolfe, J.M., Horowitz, T.S.: What attributes guide the deployment of visual attention and how do they do it? *Nature reviews neuroscience* **5**(6), 495–501 (2004)
- [60] Wu, H., Li, D., Chen, B., Li, J.: Longvideobench: A benchmark for long-context interleaved video-language understanding. *Advances in Neural Information Processing Systems* **37**, 28828–28857 (2024)
- [61] Xiao, J., Shang, X., Yao, A., Chua, T.S.: Next-qa: Next phase of question-answering to explaining temporal actions. In: *Proceedings of the IEEE/CVF conference on computer vision and pattern recognition*. pp. 9777–9786 (2021)
- [62] Yang, A., Li, A., Yang, B., Zhang, B., Hui, B., Zheng, B., Yu, B., Gao, C., Huang, C., Lv, C., et al.: Qwen3 technical report. *arXiv preprint arXiv:2505.09388* (2025)
- [63] Yang, A., Yu, B., Li, C., Liu, D., Huang, F., Huang, H., Jiang, J., Tu, J., Zhang, J., Zhou, J., et al.: Qwen2.5-1m technical report. *arXiv preprint arXiv:2501.15383* (2025)
- [64] Zhang, B., Li, K., Cheng, Z., Hu, Z., Yuan, Y., Chen, G., Leng, S., Jiang, Y., Zhang, H., Li, X., et al.: Videollama 3: Frontier multimodal foundation models for image and video understanding. *arXiv preprint arXiv:2501.13106* (2025)
- [65] Zhou, J., Shu, Y., Zhao, B., Wu, B., Xiao, S., Yang, X., Xiong, Y., Zhang, B., Huang, T., Liu, Z.: Mlvu: A comprehensive benchmark for multi-task long video understanding. *arXiv e-prints* pp. *arXiv-2406* (2024)
- [66] Zhu, J., Wang, W., Chen, Z., Liu, Z., Ye, S., Gu, L., Tian, H., Duan, Y., Su, W., Shao, J., et al.: Internvl3: Exploring advanced training and test-time recipes for open-source multimodal models. *arXiv preprint arXiv:2504.10479* (2025)
- [67] Zohar, O., Wang, X., Dubois, Y., Mehta, N., Xiao, T., Hansen-Estruch, P., Yu, L., Wang, X., Juefei-Xu, F., Zhang, N., et al.: Apollo: An exploration of video understanding in large multimodal models. In: *Proceedings of the Computer Vision and Pattern Recognition Conference*. pp. 18891–18901 (2025)

A Appendix

The appendix is arranged as follows -

1. Limitations
2. Applications
3. Data curation for universal quantizer

B Limitations.

Limitations. The main limitation is that this work only considers four complexity attributes. We believe that the space of the latter is much higher dimensional. In this sense, the current version of VideoABC is simply a starting point for additional research. We have also only used VideoABC to perform a preliminary characterization of benchmark complexity, as the main goal of the work was to introduce and test the VideoABC measure itself. We leave these extensions for future exploration.

C Applications.

Benchmark Composition. Figure 8 presents average EABC per attribute of six widely used benchmark datasets, showing how different benchmarks pose challenges along different attribute dimensions. For example, LongVideoBench is very challenging in terms of non-event proportion (due to the long videos) but not in terms of event location or scene complexity. This finding suggests that adding more challenging videos along these attribute dimensions would lead to an overall more challenging benchmark. More broadly, the figure shows some interesting observations about the benchmark landscape. First, no benchmark is most challenging across all attribute directions. MLVU has the most challenging event locations and scene complexities, while LongVideoBench dominates the non-event proportion attribute, and Egoschema the event speed attribute. Second, most benchmarks are much less challenging than the rest of the pack along at least one attribute. MLVU stands out as an exception, exhibiting a more balanced distribution, with its complexity stemming from all considered attributes. Finally, current benchmarks tend to emphasize videos that are complex in terms of non-even proportion and event speed. However, the coverage of challenging event locations and scenes is much weaker. This highlights the need for benchmarks that better capture diversity across these overlooked dimensions.

Levels of benchmarks. With the rapid advancement of video-LLMs, a growing number of benchmarks have been introduced, making comprehensive evaluation increasingly computationally expensive [67]. We show that VideoABC can effectively address this challenge by distilling large benchmarks into structured levels of difficulty. In this work, we construct five such levels, each comprising 200 samples, with the objective of maximizing the presence of videos that are simultaneously complex across all attributes. Specifically, we threshold VideoABC scores and curate a compact subset of 200 samples from Real-Bench for each level. To evaluate the effectiveness of this approach, we benchmark several video-LLMs on these distilled subsets. As shown in Table 4 (right), model performance consistently declines as the benchmark level increases, indicating that higher levels indeed correspond to more challenging samples. In conclusion, our results demonstrate

Video-LLM	Level 1	Level 2	Level 3	Level 4	Level 5
Random	0.25	0.25	0.25	0.25	0.25
Medium size					
Qwen-3.5-VL _(9B)	0.69	0.58	0.53	0.47	0.36
LLaVA-OV _(7B)	0.72	0.64	0.67	0.49	0.41
Video-LLaVA _(7B)	0.65	0.59	0.51	0.39	0.32
LLaVA-Next _(7B)	0.66	0.53	0.48	0.36	0.29
Small size					
Qwen-3.5-VL _(4B)	0.58	0.52	0.41	0.43	0.24
LLaVA-OV _(0.5B)	0.60	0.58	0.38	0.36	0.26

Training type	LLaVA-OV _(0.5B)	Qwen-3.5-VL _(4B)
Untrained	0.43	0.57
Random	0.49	0.59
Judge	0.53	0.47
MLP-A	0.49	0.56
MLP-2L	0.47	0.59
Direct	0.53	0.61
Random	0.49	0.59
VideoABC	0.57	0.63

Table 4: (Left) Performance of a LLaVA-OV (7B) model on Real-Bench with 5 levels. A random chance can secure an accuracy of 0.25 in both cases. (Right) Performance of a LLaVA-OV (0.5B) model on Eval-00D. Model is trained on Next-QA training set.

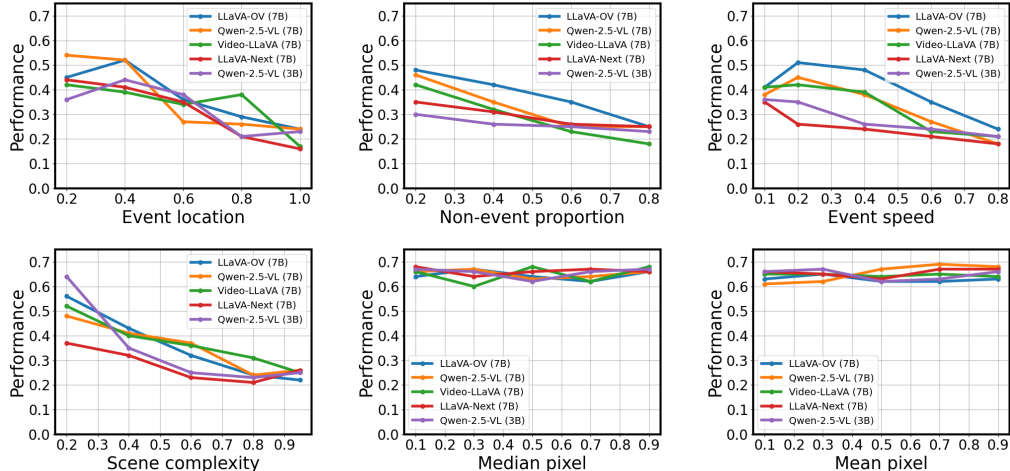


Figure 9: Figure shows sensitivity of video-LLM.

that VideoABC enables efficient and effective benchmark distillation while preserving meaningful gradients of difficulty.

Curriculum training. We consider performing supervised fine-tuning (SFT) using a curriculum defined by VideoABC. Simply we train the model first on easier questions and then on harder questions defined by different complexity score baselines. We trained LLaVA-OV (0.5B) and Qwen-3.5-VL (4B) on training set of Next-QA and measured model performance on level 5 of our curated dataset. Results are shown in table 4 (left). It can be noted that both methods trained on our method shows much better results as compared to other baselines implying our curriculum is better as compared to standard one.

Video-LLM sensitivity. A complementary question is how sensitive is video-LLM performance to complexity along the various attribute dimensions. To investigate this, we leveraged the universal quantizer to measure model performance p as a function of the complexity of each attribute a , while maintaining the remaining constant. Given the values c_j of the attribute bin centers and the associated EABCs average model performance $p_j = 1 - \psi_j^u$, the model sensitivity was measured with $s_j = (p_{j+1} - p_j) / (c_{j+1} - c_j)$. Figure 9 shows the model sensitivity of video-LLMs towards different attributes. Two conclusions can be made. To begin with, event speed attribute breaks most of video-LLMs at a lower complexity value while for other attributes, it is at some higher complexity value. The main reason for such a behavior is the lack of essential frames to answer the question. Event speed and scene complexity are primary factors and that is because the model is unable to get relevant frames to answer questions. Overall, the most effective attribute at breaking video-LLMs is event speed followed by scene complexity. Furthermore, it can be noted that model size is another contributing factor preventing model’s breakage. However, it is effective for only non-event proportion and frame difficulty. For other attributes such as event speed, model size does not seem to be a solution. Overall, it shows that certain attributes are more effective at breaking video-LLM and there is a need to have video-LLM architectures that can resolve these.

D Data curation for universal quantizer.

VideoABC-Bench is a new benchmark for studies of how complexity attributes affect video-LLM performance. It is inspired by the well established protocols for the study of visual attention [10, 18, 27, 43, 54, 35], relying on a video dataset of simple but controllable objects, namely colored balls and squares displayed against a white background, as shown in Figure 10. Both balls and squares are subject to attribute changes, *e.g.* a change of size or color.

The main benefit of VideoABC-Bench over benchmarks of real video is that each attribute can be manipulated *independently*. This is important to show that the attribute can, *by itself*, determine video complexity. In every experiment of the current implementation of VideoABC-Bench, the target object is a green ball. The video-LLM is asked a question q grounded on an event $\mathcal{E}(q)$, which is an *attribute change* of the target, *e.g.* color in Figure 10 (a), and presented with 5 possible answers. All

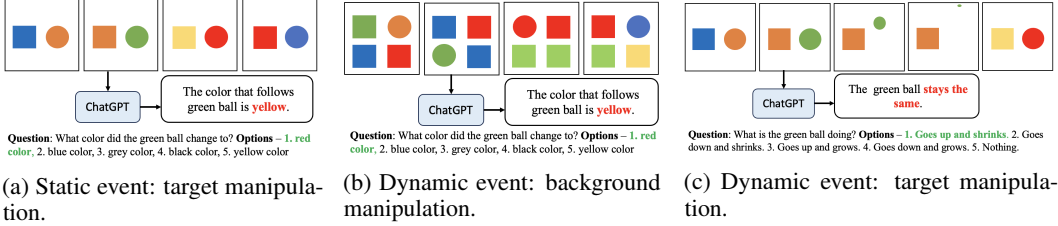


Figure 10: Different types of events of VideoABC-Bench.

remaining squares in the video serve as distractors that increase the difficulty of detecting the event. Two types of events are defined and a pair of target and distractor manipulations defined for each.

Static events. In these events, the target manipulation involves switching the value of a static attribute, namely the color, of the target. As shown in Figure 10 a) the event \mathcal{E} is a change of the color of the green ball at a unique *event location* (frame pair) in the video. The remaining balls and squares are chosen randomly (restricting ball colors to non-green) per frame pair. The target manipulation consists of varying the *event location* in the video. This can be a) beginning of video, $j \in [0, 2\gamma]$, b) middle of video, $j \in [4\gamma, 6\gamma]$ and c) end of video, $j \in [8\gamma, 10\gamma]$. The task is defined by a question that asks the video-LLM to choose the new color of the ball from 5 options. In the example of Figure 10 a) the correct answer is 'red'. The distractor manipulation consists of varying the *non-event length*, by concatenating frames at the end of the video, so that $N \in [10\gamma, 120\gamma]$. As the video length increases, the event becomes more of a needle in haystack, and the task is harder.

Dynamic events. In this case, the target manipulations are dynamic, namely the combination of (upward or downward) ball motion and variation (increase or decrease) of ball size. Figure 10 c) shows an example where the ball moves up and shrinks. The task is to choose from one of the four possible combinations of motion and shape change plus the 'none of the above' option. The distractor manipulation consists of increasing the *number of distractors*. This allows the appearance of the entire scene to change across frame pairs, creating a dynamic background and increasing the difficulty of finding the target, especially as the number of distractors grows, as illustrated in Figure 10 b). The target manipulation is to increase the *rate of change of the target*. This is implemented by varying the *frame rate* γ . Given an event frame rate γ_E , the Nyquist rate $\gamma_N = 2 \times \gamma_E$ is a lower bound for the video frame rate, in the sense that for any $\gamma < \gamma_N$ it should be hard to understand the video even for a human. We used $\gamma_E = 2$ and varied γ between 1 and 32. The event position is always at the beginning of video ($j \in [0, 2\gamma]$) in these experiments.

Overall, the VideoABC-Bench currently allows *independent* control of four *attributes of video complexity*: event location \mathcal{A}_1 , surrounding (non-event) video length \mathcal{A}_2 , scene complexity (number of distractors) \mathcal{A}_3 , and event speed (frame rate) \mathcal{A}_4 . These are proxies for real video event attributes such as the length of an informative action versus the length of the video, action speed, or the complexity of the background scene. While these properties are difficult to control in real videos, the hypothesis of the paper is that these attributes affect *temporal complexity* and thus video-LLM performance. VideoABC-Bench allows detailed studies of this hypothesis. Note that we make no claims that these are the only complexity attributes of video. In fact, we propose VideoABC-Bench as an evolving benchmark, to which other researchers interested in studies of video complexity can add different attribute hypothesis.

Dataset. VideoABC-Bench comprises 1200 video-question pairs, with 700 featuring static events and 500 containing dynamic events, generated as follows. For static events, 300 videos include target manipulations, where the event is equally distributed between beginning, middle and end of the video. For distractor manipulation, 400 videos were generated with length $N \in \{20, 40, 60, 80\}$, with 100 videos per video length. For dynamic events, target manipulations are based on 100 videos with frame rate of 2 fps. The manipulations consisted of adjusting the fps setting of the video-LLM to a value $\gamma \in \{0.8, 1.6, 3.2, 4.8, 6.4, 8\}$. For distractor manipulations, 400 videos were created with $D \in \{1, 2, 3, 4\}$ distractors, with 100 videos per category.